Structures and Redox Characteristics of Electron-Deficient Vanadyl Phthalocyanines

ARTICLE *in* INORGANIC CHEMISTRY · APRIL 2011

Impact Factor: 4.76 · DOI: 10.1021/ic2000365 · Source: PubMed

Inorganic Chemistry

ARTICLE

pubs.acs.org/IC

Structures and Redox Characteristics of Electron-Deficient Vanadyl Phthalocyanines

Łukasz Łapok,[†] Martin Lener,[‡] Olga Tsaryova,[†] Stefanie Nagel,[‡] Christopher Keil,[‡] Robert Gerdes,[†] Derck Schlettwein,[‡] and Sergiu M. Gorun*[,†]

[†]Department of Chemistry and Environmental Science, New Jersey Institute of Technology, Newark, New Jersey 07102, United States

[‡]Institute of Applied Physics, Justus-Liebig-University Giessen, Heinrich-Buff-Ring 16, D-35392 Giessen, Germany

Supporting Information

ABSTRACT: The first single-crystal X-ray structures of substituted vanadyl phthalocyanine materials reveal the high-valence vanadium ions (denoted as V(IV)), whose coordination by a highly electron-deficient ligand is facilitated by an axial oxo group. The metal center of the hydrophilic V═O core, encapsulated in F-rich hydrophobic pockets, reaches a coordination number of 6 by binding an additional H_2O that, in turn, hydrogen-bonds with ketones, resulting in solvent-induced variable solid-state architectures. Fluoroalkyl (R_f) ligand substituents hinder $\pi-\pi$ stacking interactions and favor ordered long-range packing, as well as the facile formation of film materials that exhibit high thermal stability and oxidation resistance. Reversible redox chemistry and spectroscopic studies in both solution and the solid-state indicate single-site isolation in both phases and an R_f-induced propensity for electron uptake and inhibition of electron loss. Repeated redox cycles reorganize the thin films to accommodate Li^+ ions and facilitate their migration. The facile reduction, combined with high stability and ease of sublimation imparted by the R_f scaffold that suppresses oxidations, recommends the new materials for sensors, color displays, electronic materials, and redox catalysts, as well as other applications.

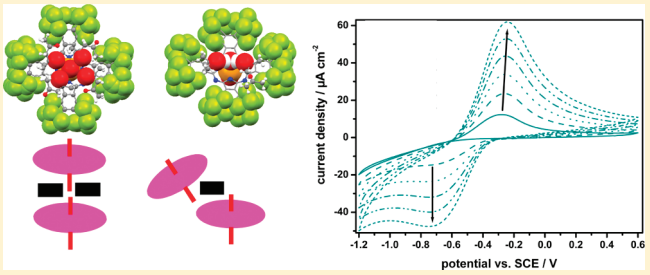

INTRODUCTION

Phthalocyanines (Pcs) have been proposed as electronic materials, based on their robustness, multiple redox states, strong light absorption, and structural and electronic tunability via classical chemistry.[1]

The absolute energy levels of Pcs frontier orbitals, as well as their gap, are critical for tuning electron transfer and energy absorption processes *at the molecular level*. Most Pcs donate electrons, since their highest occupied molecular orbitals (HOMOs), ascribed to the aromatic π-system, have the appropriate high energy. Electron-donating substituents further increase the energy of the frontier orbitals, thus facilitating oxidation and suppressing reduction. Electron-withdrawing substituents have the opposite effect, leading to more-negative values of the lowest unoccupied molecular orbital (LUMO) energies and, thus, facile reduction. The halogenation of Pc rings, resulting in the formation of, for example, $F_{16}PcM$ (M = metal) complexes, illustrates this point: *n*-type semiconduction is observed in their thin films.[2] Organic groups attached at the periphery of Pc rings could also sterically modulate intermolecular interactions, including $\pi-\pi$ stacking, thus influencing the formation process and structure of thin films, required for other organic-material-based applications such as photovoltaic cells (OPVs),[3] light-emitting diodes (OLEDs),[4] and field-effect transistors (OFETs).[2] The combination of film-forming ability in the 10−100 nm range and variable redox states with high molar extinction coefficients (intense colors) renders Pcs candidates for electrochromic devices.

Practical applications based on redox chemistry, however, impose additional constraints, such as a high degree of electrochemical reversibility and fast redox changes, as well as thermal inertness and resistance to environmental challenges, especially oxidations. An important parameter is the ability of films to facilitate the migration of charge-neutralizing counterions upon oxidation or reduction, with ion transport usually being the rate-limiting step of redox processes in the solid state.

We have recently reported a new class of divalent metallophthalocyanines whose extreme electron deficiency is imparted by a 1:1 combination of aromatic F and *iso*-perfluoro alkyl (*i*-R_f) groups, viz. perfluoro *iso* propyl, C_3F_7 groups.[5] The formal replacement of eight aromatic F atoms in $F_{16}Pc$ by eight R_f groups to yield $(R_f)_8F_8PcM(II)$ molecules diminishes the overall π-back bonding effect, further depresses the PcM frontier orbitals,[6] and enhances the chemical and thermal stability of Pcs (for M = Co, Zn, Cu), as well as the photostability of the complexes, even under conditions where reactive singlet oxygen is produced (for M = Zn).[7] The *iso* nature of the R_f groups ensures the formation of isolated, single-site catalysts[7] and chromophores by suppressing aggregation

Received: January 6, 2011
Published: April 05, 2011

as seen in the single-crystal X-ray structure for M = Zn, Co, Cu. Consequently, the electronic and magnetic intermolecular coupling is blocked, as revealed by concentration-independent optical spectra that strictly obey the Lambert−Beer law (M = Cu, Zn, Co), concentration-independent ^{19}F NMR spectra (M = Zn, Cu), single-site isolated ESR signals (M = Cu),[8] and a strict following of the Curie law (negligible Weiss temperature, M = Cu).[8] In addition, low conductivity in the solid state has been noticed for M = Cu, Zn, VO.[5e] The Pcs with M(II) exhibit additional axial solvent coordination in solution and in the crystalline state (for example, acetone, methanol, ethyl acetate, and acetonitrile), as well as ligands whose unique functional group is metal-bonded while their hydrocarbon moieties further hinder aggregation. However, physical deposition of PcM(II) under high vacuum conditions, results in the loss of axial ligands, leaving the metals four-coordinated and, thus, at least in principle, increasing the chances of solid-state aggregations in films.[5e]

In contrast, for M = V(IV)O (vanadyl), the axially coordinated oxo group cannot be removed without an increase in the formal metal charge from +2 to +4. Given the reduced Lewis basicity of the coordinating N atoms imparted by the R_f groups, this change of oxidation state is deemed unlikely. On the other hand, the stable $[V(IV)O]^{2+}$ ion that formally exhibits a lower charge allows the formation of a five-coordinated $(R_f)_8F_8$PcV=O complex, F_{64}PcVO.[5e] The metal center may still bind additional Lewis bases, similar to F_{64}PcM(II) complexes, but, unlike them, the fifth ligand, the oxo group, could, in principle, favor aggregation or surface binding. As an example, magnetic interactions between films containing paramagnetic PcV=O and the (001) surface of semiconducting GaAs has been reported very recently, as a prerequisite for single-molecule-based spintronics.[9]

We report here the single-crystal X-ray structures of two solvated F_{64}PcVO compounds. These are the first structurally characterized substituted PcVOs, materials whose solid-state architecture, aggregation, and film-forming properties are modulated by an increase in the metal coordination number to six, by solvation and hydrogen bonding, as well as by the effects of R_f substituents. We also report redox and electrochemical properties of the complex in solution and solid-state and the relevance of the structural information to these properties.

MATERIALS AND METHODS

All reagents were obtained commercially and used without purification, unless stated otherwise. 1,4,8,11,15,18,22,25-octakis-fluoro-2,3,9,10,16,17,23,24-octa-perfluoroisopropyl phthalocyaninato vanadium(IV) oxide, F_{64}PcVO was synthesized and purified as briefly reported recently.[5e] Single crystals in two morphologies were obtained via the slow evaporation of saturated solutions at room temperature. The quality of the crystals reported earlier has been improved significantly through the use of either pure acetone or a large excess of methyl ethyl ketone for crystallization. Single-crystal X-ray data were collected at a temperature of 100 K on a Bruker SMART APEX CCD diffractometer, using Cu Kα radiation (1.54178 Å). The structures were solved using direct methods and refined using a full-matrix least-squares methodology on F^2, employing the SHELXTL package.[10a,b] Additional structural calculations were performed using PLATON.[10c] Structural searches were performed using the Cambridge Structural Database.[10d] Cyclic voltammetry (CV) was performed for saturated solutions of F_{64}PcVO in trifluorotoluene (TFT) with tetrabutyl ammonium tetrafluorborate ($TBABF_4$) as the supporting electrolyte, using platinum wires as working and counter electrodes and an additional platinum wire as quasi-reference electrode with ferrocene as a post-measurement internal standard at +0.4 V vs SCE. Spectroelectrochemical measurements were performed using platinum-plated glass plates as working and counter electrodes in a quartz cell. Alternatively, thin films of F_{64}PcVO vapor-deposited at ∼0.5 nm/min on ITO-covered glass were used for solid-state CV as the working electrode in contact with 1 M solution of LiCl in doubly deionized water, with a Ag/AgCl reference electrode and a platinum counter electrode. A diode array spectrometer (Tec5 LOE-MMS1) was connected by optical fibers to probe changes in the absorption spectrum.

RESULTS AND DISCUSSION

Vanadyl phthalocyanine (H_{16}PcVO) was reported 75 years ago.[11] The complex and its ring-substituted derivatives found use as pigments, semiconductors, photoconductors, photoreceptors, imaging agents, and catalysts. These and other potential applications triggered academic and industrial research efforts.[1−4] Three crystalline phases—α, β, and γ—were identified for H_{16}PcVO 35 years ago.[12] Dimeric structures have been suggested for all phases, but only the β phase was characterized, 30 years ago, via a single-crystal X-ray structural determination.[13] The formation of dimeric assemblies takes place via intermolecular contact of the benzene rings below the 3.6 Å threshold that is indicative of π−π interactions.[14] The X-ray structures of substituted PcVOs have not been reported, although several PcVOs substituted with *t*-butyl,[15a] variable-size alkoxy groups,[15b,c] or hexyloxyl groups,[15d] yielded solid-state materials ranging from amorphous to crystalline to liquid crystalline.

The X-ray structural characterization of substituted vanadyl phthalocyanine that we report here was facilitated, somewhat unexpectedly, by the ability of fluorine groups to support crystallization of molecules.[16] The finding that a metal in a high-valence state (+4, denoted as IV) can be accommodated in an electron-deficient coordinating environment is also surprising, but it can be rationalized by the presence of the axial oxo ligand.

The structures of F_{64}PcVO·(H_2O)·solvent complexes are shown in Figure 1. For complexes **1** and **2**, the solvents of crystallization are acetone (three molecules) and methyl−ethyl ketone (MEK) (four molecules), respectively. The difference of a single methyl group had a dramatic effect on the solid-state architecture of the materials (see Figures 1e−i).

The main structural feature of F_{64}PcVO (Figures 1a and 1b) is similar to that of related macrocyclic vanadyl complexes, namely, a five-coordinated metal center displaced from the ligand plane. The additional H_2O coordination (Figure 1b) is an unprecedented feature for Pcs, although it was postulated to occur in frozen dimethyl sulfoxide (DMSO) solutions of *t*-butyl PcVO as a possible alternative to DMSO coordination.[17] Ketone molecules (Figures 1c and 1d) are embedded in the fluorinated pocket of the faces bearing the H_2O in F_{64}PcV=O·(H_2O). The $O(H_2O)\cdots O$(carbonyl of acetone) distances for **1** are 2.809(5) and 2.763(4) Å, values that are close to the 2.8(1) Å mean of the 2.55−2.95 Å range observed for all metal−$H_2O\cdots$acetone hydrogen-bonding contacts.[10d] (also see Figure S3 in the Supporting Information for a statistical analysis). The similar distances for **2**—3.104(7) Å and 2.829(6) Å—cannot be discussed statistically, since only one other molecule, an aqua ruthenium complex,[18] which exhibits a metal−$H_2O\cdots O$(MEK) contact of 2.67 Å seems to have been reported.[10d] Hydrogen bonding, albeit

dx.doi.org/10.1021/ic2000365 |*Inorg. Chem.* 2011, 50, 4086–4091

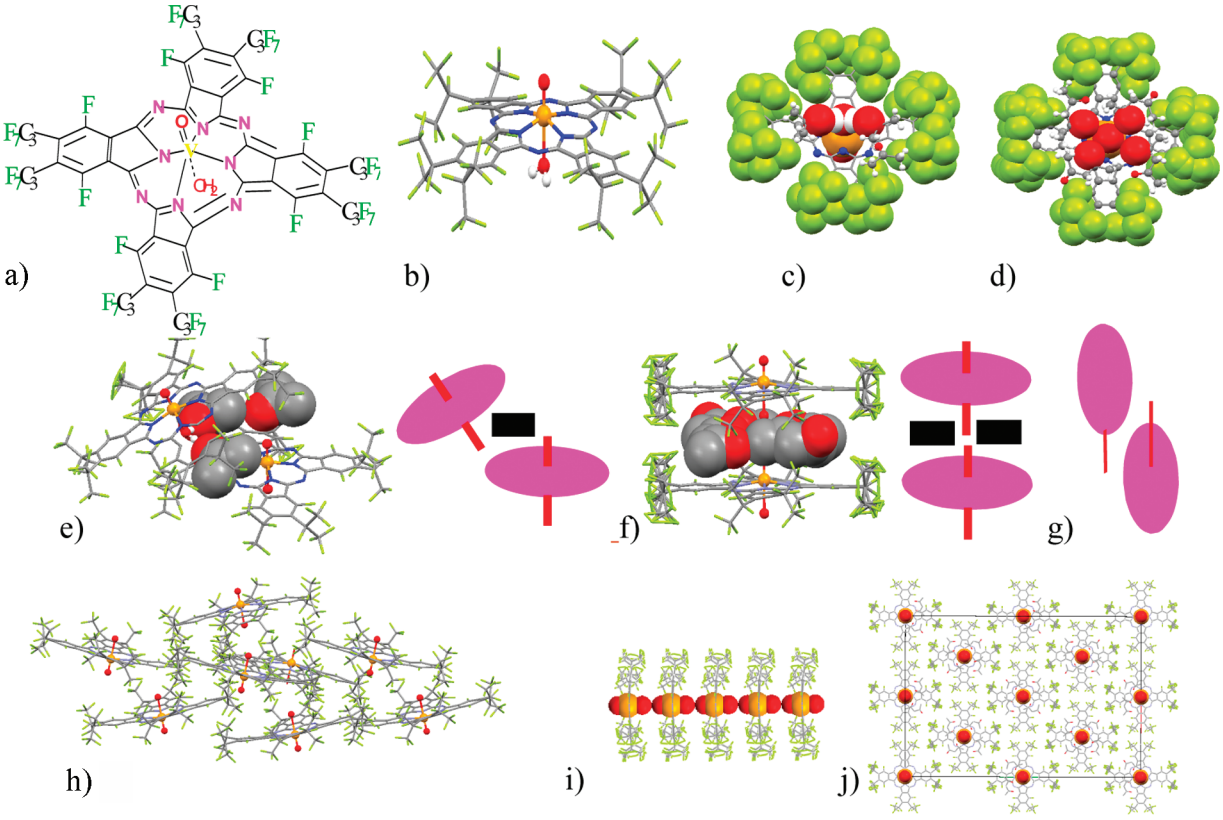

Figure 1. Structures of orthorhombic **1** and **2**. Color code: V, orange; O, red; N, blue; F, green; C, gray; and H, white. (Most H atoms have been omitted, for the sake of clarity.) (a) Structural formula of the common $F_{64}PcVO\cdot(H_2O)$ moiety. (b) Single-crystal X-ray structure of the $F_{64}PcVO\cdot(H_2O)$ unit; the V, oxo, and H_2O groups are shown as balls and sticks. (c) The structure of $F_{64}PcVO\cdot(H_2O)\cdot 3$(acetone), **1**; the V, F, oxo, H_2O, and carbonyl groups of the two hydrogen-bonded acetone molecules are shown as van der Waals spheres. (d) The structure of $F_{64}PcVO\cdot(H_2O)\cdot 4$MEK (where MEK denotes methyl ethyl ketone) (**2**); the V, F, oxo, H_2O, and carbonyl groups of the four hydrogen-bonded ketone molecules are shown as van der Waals spheres. (e) Assembly of two adjacent $F_{64}PcVO\cdot(H_2O)$ units in **1**, tilted by 25° by the three acetone molecules, which are shown as van der Waals spheres. In the schematic representation, the solvents are depicted as a black rectangle. (f) Assembly of two adjacent $F_{64}PcVO\cdot(H_2O)$ units in **2**. The architecture is modulated by the four MEK molecules (shown as van der Waals spheres). Schematic representation showing the solvents depicted as black rectangles. (g) Schematic representation of the shortest-contact "dimers" present in the layered structure of β-$H_{16}PcVO$. (h) Packing diagram of **1**. (i) Packing diagram of **2**. (j) Columnar stacking in **2**, showing the one-dimensional $-H_2O-V{=}O-H_2O-V-O-H_2O-V{=}O-$ central assembly.

weaker, relative to **1**, seems to be present in **2** as well, assisted perhaps by H(MEK)···(Pc) interactions.[16] The 3.104(7) Å contact probably is slightly too long to qualify as a hydrogen bond.

For both **1** and **2**, the observed hydrogen bonding illustrates the presence of highly hydrophilic metal-aqua centers on one face of the molecule, within a very hydrophobic R_f environment. This extreme architecture actually is favored electronically by the R_f groups that render the metal center highly Lewis acidic. The *trans* oxo group provides a similar hydrophilic environment on the opposite face of the R_f Pc.

The *intramolecular* structural effects of R_f groups and hydrogen bonding on the axial ligands have been examined. For **1** [and **2**, the V−O(H_2O) and V═O distances are 2.359(3) [2.358(6)] Å and 1.586(3) [1.539(7)] Å, respectively. The V═O distance in $H_{16}PcVO$ (1.580(3) Å) is similar to the average V═O bond length in **1** and **2** (1.562(7) Å), but is much closer to the value of **1** (1.586(3) Å). A structural analysis of all *trans* O═V−H_2O moieties[10d] is presented in Figure 2. The sum of the *trans* metal−oxygen distances correlate well ($R = 0.98$) with the V−O(H_2O) distances (but not with V═O distances; see Figure S3 in the Supporting Information) with a unit slope, thus indicating that the V═O distance (1.593(3) Å) is statistically insensitive to changes in the metal coordination environments, hydrogen bonding, and even the presence of a positive charge on a porphyrin (Por) ligand. The linear equation was fitted *without* considering the data for $Por^{+}VO(H_2O)$, as well as **1** and **2**, thus suggesting that the V═O bond in **2** is unusually short, and that this fact is not due to a *trans* effect. A sensible explanation must await the structural characterization of more Pc and Por vanadyl complexes.

With the exception of V═O distances, **1** and **2** exhibit similar structural features of their $F_{64}PcVO$ moieties. The V−N distances—2.027(4) and 2.033(4), respectively—are statistically indistinguishable. The doming of the Pcs is virtually identical, with the V−N_4 (coordination plane) distances being 0.36(1) Å in both cases. The benzene rings are twisted by less than 10°.

The *intramolecular* structural effects of fluorination are apparent in a comparison of the average parameters of **1** and **2** with those of the parent, nonfluorinated $H_{16}PcVO$ complex [data in brackets]. Although the V−N distance, 2.030(4)[2.026(7)] and, as shown in Figure 2, the V═O distances appear similar, the V is 0.2 Å closer to the N_4 coordination plane in **1** and **2**, a reflection of the 0.1 Å elongated opposite N···N distances, which reach 4 Å for **1** and **2**. Thus, the metallo-macrocycle ring in **1** and **2** counterintuitively deviates less from planarity here than in $H_{16}PcVO$, despite an increase in the steric bulkiness of the peripheral substituents. This effect could be ascribed to an increase in the ligand

dx.doi.org/10.1021/ic2000365 |*Inorg. Chem.* 2011, 50, 4086–4091

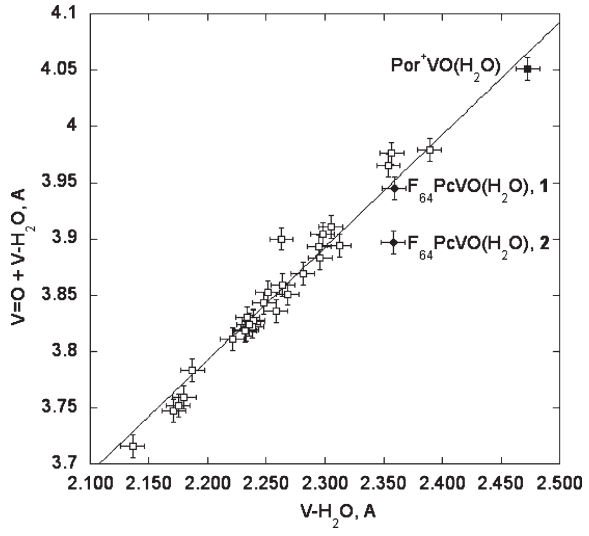

Figure 2. Variation of the sum of axial V−O distances vs the V−O(H_2O) distances for all *trans* O═V−O(H_2O) units.[10d] The linear correlation equation is $y = x + 1.593(3)$. The error bars reflect the average three estimated standard deviations (esd) values in the bond lengths.

coordination sphere and approximate invariability of the V−N bond lengths, despite a formal change in coordination number (CN) from five in the parent compound to six in **1** and **2**. In contrast, DFT geometry optimization of tetramethoxy PcVO lead to the conclusion that the substituents have no significant structural effects, relative to H_{16}PcVO.[15d]

The combined *intermolecular* structural effects of R_f groups and solvation, unlike the *intramolecular* effects, are significant. Solvation could be important for applications materials chemistry; a redox active solvent stabilizes the aggregation of H_{16}PcVO, which is a feature deemed critical for designing photoconductive materials.[19]

First, for F_{64}PcVO(H_2O), the degree of solvation varies. Complex **1** binds three ketone molecules, whereas **2** binds four. Since the degree of solvation is smaller for the smaller ketone (acetone vs MEK), one could conclude that additional packing forces influence the solvation process. It is difficult to determine if the tilt of the Pc rings in **1** (see Figure 1e) causes the intercalation of a layer of acetone, or vice versa. In both **1** and **2**, the ketones are disordered while hydrogen-bonded to the coordinated H_2O. MEK seems to have a higher affinity for the complex, since **2** was obtained from a 1:1 v:v mixture of acetone:MEK. The tilt in **1** results in a classical, herringbone-type crystalline long-range order (see Figures 1e and 1h). In the case of **2**, the molecules form a columnar stack (see Figures 1f, 1i, and 1j). Unlike the case of β-H_{16}PcVO (Figure 1g), where packing forces include (benzene ring−benzene ring) $\pi-\pi$ stacking interactions at 3 Å, the bulky R_f groups of **1** and **2** prevent stacking. On the other hand, they introduce F···F interactions that might contribute to the tilt in **1** and intercolumnar stacking in **2** (Figure 1j).[5a−d,16]

The two modes of assembly result in different interstitial volumes for potential solvent occupancy. We have estimated the volumes of potential solvent-accessible voids for **1** and **2**, assuming that the ketones, but not the H_2O, are either present or missing.[10c] Thus, the accessible volumes for **1** and **2** are 1125 (7% of the unit cell) and 0 Å^3, respectively. If the ketones are removed, the volumes become 4074 (25% of the unit cell) and 4748 (28% of the unit cell) Å^3, respectively. The packing plasticity, which is induced by volatile solvents likely to be lost in the solid state, suggests low-energy intermolecular interactions. Indeed, the R_f groups impart favorable volatility properties. Compared to the parent H_{16}PcVO that decomposes in air at 350 °C and sublimes under vacuum above 365 °C, F_{64}PcVO sublimes at 280 °C without decomposition.[5e] This technological advantage of an 80° decrease in the sublimation temperature occurs despite the 3.5 fold increase in molecular weight. The diminished R_f-induced intermolecular interactions and the consequent loose packing in the solid state suggested opportunities for film formation,[5e] as well as the possibility of cation intercalation in interstitial spaces. Note that a tight packing, such as that observed for the β-phase of H_{16}PcVO, prevents the intercalation of cations upon electrochemical reduction.[20] The α-phase, in contrast, which is presumably less tightly packed, allows cation penetration and, thus, solid-state reductions that result in color changes upon reduction (electrochromic effect).

Since the packing forces present in **1** and **2** are weak and the solvent can be removed to yield films in which the molecules are randomly oriented,[5e] we have probed the solid-state effects of the R_f groups by examining the solid-state redox properties of evaporated films of **1** and **2** (see below). The lack of conductivity of the F_{64}PcVO films[5e] casted an initial doubt on the possibility of redox activity in the solid-state. On the other hand, R_f groups enhance the electron affinity of **1** and **2** in solution, while facilitating the formation of both well-defined crystals and films.

The R_f groups, which narrow the HOMO−LUMO gap, shift the absorption spectrum of F_{64}PcVO (in ethyl acetate) slightly, relative to the parent H_{16}PcVO and even F_{16}PcVO.[15c,21] Major absorption bands are observed at the following λ (nm) (log ε) values: 693 (5.31), 625 (4.64), 387 (4.83). In addition to exhibiting a narrowed frontier orbital gap, the orbital energies of F_{64}PcVO are also depressed, as illustrated by the redox chemistry (Figure 3a). Thus, for F_{64}PcVO, three reduction and reoxidation waves are detected in TFT solutions. The redox potentials of 0.00, −0.38 V (vs SCE) are ascribed to the reduction of Pc^{2-} rings to $Pc^{3-\bullet}$, as indicated by the growth of a new absorption band at 595 nm, characteristic for $Pc^{3-\bullet}$, at the expense of the ∼690 nm Q-band. Redox characteristics that were almost identical to those reported in Figure 3a were also observed in a study of the M(II) complexes, namely, F_{64}PcZn and F_{64}PcCu. The spectral changes observed there occurred continuously across the redox waves I and II, starting already in the positive range, indicating a simple $Pc^{2-} \rightarrow Pc^{3-\bullet}$ redox step, despite two observed redox waves.[22] In those cases, the metal center, especially Zn(II), is irreducible and, thus, the reductions are unambiguously assigned to the Pc ligand. The existence of two waves for the first redox step under continuous spectral change suggests molecular association, unlikely to be of the $\pi-\pi$ type, because of steric hindrance, but consistent with the high electron affinities of the complexes. Association is favored in highly concentrated (saturated) solutions as used in the electrochemical experiments, but the stabilization of the additional charge and radical character via molecular association is not strong enough to result in an independent UV−vis spectroscopic signature.[22] Notably, in the case of the M(IV) complex reported here, and unlike the cases of M(II) complexes, an oxyl group provides additional opportunities for association, as suggested by the packing diagram of **2** (see Figure 1i).

The third potential (−1.12 V) is ascribed to the further reduction of $Pc^{3-\bullet}$ to Pc^{4-}. The fourth reduction wave is partially masked by the increasing background current near the negative end of the scan.

dx.doi.org/10.1021/ic2000365 |*Inorg. Chem.* 2011, 50, 4086–4091

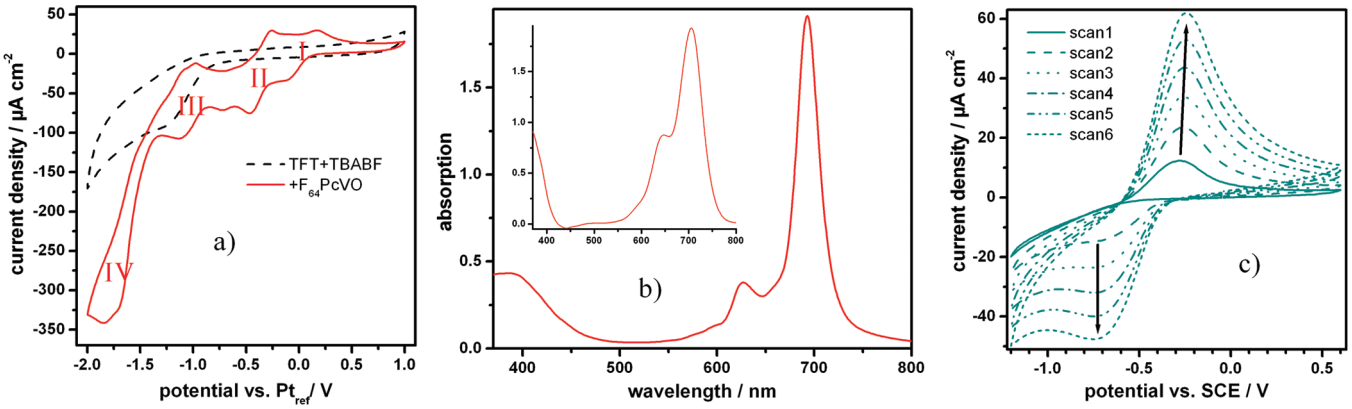

Figure 3. The redox chemistry of F_{64}PcVO. (a) CV, solution; scan rate = 100 mV s^{-1}, redox potentials of 0, −0.38, and −1.12 V vs SCE for reductions I, II, and III, respectively. (See the text for details.) The background CV is shown as a dashed trace. (b) UV−vis absorption in solution. Inset shows absorption in the solid state (film). (c) Repeated CV scans in the solid state of a 215-nm film (scan rate = 0.3 V s^{-1}).

Both the solution and solid-state redox properties of fluorinated PcVOs are critically dependent on the type of fluorine substituent. Thus, F_{16}PcVO exhibits more-negative redox potentials, −0.29 and −0.62 V (in CH_2Cl_2), relative to F_{64}PcVO, but lacks a third reduction wave.[15c] Importantly, an *oxidation* process, observed for F_{16}PcVO at +1.34 V (vs SCE), is absent in F_{64}PcVO. The difference, including the onset of oxidation protection is due to the formal replacement of eight aromatic F groups of F_{16}PcVO by R_f groups and the consequent removal of eight π-back-bonding interactions. F_{16}PcVO also exhibits H_{16}PcVO-type polymorphism in films deposited on various surfaces and does not form materials suitable for single-crystal X-ray diffraction.[23]

Thin solid films of F_{64}PcVO exhibit Q bands similar to those observed in solution (Figure 3b). Spectral broadening was observed as reported earlier for such films,[5e] but no splitting of the transitions caused by intermolecular coupling is observed. These observations are consistent with the lack of a spectral signature, in the case of molecular association noted previously for both M^{2+}, CN = 4 (M = Zn, Co) and reported above now for M^{4+}, CN = 5 or 6 (M = V).[21b,24]

The CV in the solid state (see Figure S4 in the Supporting Information) reveals a redox cycle with $E_{1/2} = -0.54$ V, which is a value that is similar to those observed for the Zn and Cu complexes.[22] A strong sample-history dependence on the degree of reduction (Figure 3c) is noticed, which is indicative of a stepwise solid-state reorganization of the films induced by Li^+ cations of the LiCl electrolyte, intercalated into the F_{64}PcVO film to compensate the charges injected upon reduction. The gradual increase in the current density suggests that ionic pathways allowing Li^+ to migrate in and out of the film are established by the electrochemical reaction. Consequently, the completeness and the degree of reversibility of the redox processes increase. Interestingly, the peak values of the E_{red} and E_{reox} parameters remain almost constant during the reorganization process, as indicated by their largely vertical alignment (see Figure 3c). This observation suggests that the redox process at each step is virtually independent of changes in intermolecular interactions that could occur during the reorganization process and that only little additional hindrance of ionic transport in the films is observed with increasing completeness of the redox reaction.

Such facile movement of Li^+ in F_{64}PcVO is favored by the bulky R_f groups, since they hinder $\pi-\pi$ stacking, which would lead to a tight solid-state packing and suppressed Li^+ migration, as seen, for example, in the β-phase of H_{16}PcVO.[20] For the latter, we calculate that there is no accessible space in the lattice, in contrast to the accessible voids in **1** and **2**. In addition to a favorable packing, one also might consider that both the central hydrophilic regions that encompass the oxo/aqua groups, as well as the F-rich Pc periphery, might provide pathways for the migration of Li^+ cations. Moreover, the weak F−F interactions and the absence of π-stacking also are likely to reduce the energy required to reorganize the films, whereas the oxo groups may have an opposite effect, with the balance of which leading to the delayed establishment of a steady-state redox process. As shown in Figure 3c, the reorganization is not reversible upon reoxidation (in other words, after the film is depleted of Li^+ cations). Thus, the new film architecture that comprises the pathways that allow facile cation transport seems to be stable. Indeed, in the case of F_{64}PcVO, the cations do not seem to encounter transport limitations, even at a thickness of 174 nm, as suggested by the linear dependency of the current density on the scan rate (see Figure S5 in the Supporting Information), in contrast to the case of F_{64}PcCu, for which limitations already exist at 73 nm.[22]

In conclusion, the first X-ray structures of substituted vanadyl phthalocyanines reveal the role of substituents in favoring the formation of both well-defined crystalline and film materials. The films exhibit thermal and R_f-induced electron-loss (oxidation) resistance. The electron-deficient phthalocyanine binds a metal in a high-valence state (IV), which is a property that is likely favored by the axial oxo ligand. The highly hydrophilic and Lewis acidic metal centers, while encapsulated in a F-rich hydrophobic environment, are hexacoordinated, because of axial H_2O binding. Hydrogen-bonded ketones nest in R_f-fluorinated pockets. The fluoroalkyl molecules exhibit solvent-induced plasticity of their solid-state architecture, with an extra methyl group in the hydrogen-bonded solvent being sufficient to induce columnar stacking. The high fluorine content, in conjunction with the steric hindrance of $\pi-\pi$ stacking, (i) favors the facile formation of films via physical vapor depositions; (ii) induces high volatility, despite high molecular weights; (iii) allows cation-induced film reorganization; and (iv) favors the reversibility of redox processes in both solution and the solid state, which is indicative of single-site isolation in both phases. The redox chemistry, combined with the high stability of the fluorinated organic scaffold that suppresses oxidations, recommends the new material for solid-state

dx.doi.org/10.1021/ic2000365 |*Inorg. Chem.* 2011, 50, 4086–4091

applications. Materials with related R_f groups are expected to exhibit similar advantages.

■ ASSOCIATED CONTENT

Supporting Information. Crystallographic tables and additional plots of the molecular structures of **1** and **2**. CCDC File Nos. 815778 and 815779 contain the full crystallographic data for this paper. The data can be obtained free of charge via http://www.ccdc.cam.ac.uk/conts/retrieving.html, or from the Cambridge Crystallographic Data Centre, 12 Union Road, Cambridge CB2 1EZ, U.K.; fax: (+44) 1223-336-033; or e-mail: deposit@ccdc.cam.ac.uk. Supporting Information for this article contains a statistical analysis of the structural parameters as well as additional plots of cyclic voltammetry and current vs scan rate. This material is available free of charge via the Internet at http://pubs.acs.org.

■ AUTHOR INFORMATION

Corresponding Author
*E-mail address: gorun@njit.edu.

■ ACKNOWLEDGMENT

The authors are grateful for financial support of parts of the work by the U.S. Army and the Justus-Liebig-University Giessen. R. Lalancette is thanked for the raw X-ray data.

■ REFERENCES

(1) (a) Leznoff, C. C., Lever, A. B. P., Eds. *Phthalocyanines: Properties, and Applications*; VCH Publishers: New York, 1996. (b) McKeown, N. B. *Phthalocyanine Materials*; Cambridge University Press: Cambridge, U.K., 1998. (c) Kadish, K. M.; Smith, K. M.; Guillard, R. *The Porphyrin Handbook*; Academic Press: San Diego, CA, 2003; Vols. 15−17. (d) Claessens, C. G.; Hahn, U.; Torres, T. *Chem. Record* **2008**, *8*, 75. (e) Brinkmann, H.; Kelting, C.; Makarov, S.; Tsaryova, O.; Schnurpfeil, G.; Woehrle, D.; Schlettwein, D. *Org. Electron.* **2009**, 37. (f) Lukyanets, E. A.; Nemykin, V. N. *J. Porphyrins Phthalocyanines* **2010**, *14*, 1.

(2) (a) Liu, S. H.; Wang, W. C. M.; Briseno, A. L.; Mannsfeld, S. C. E.; Bao, Z. N. *Adv. Mater.* **2009**, *21*, 1217. (b) Zhang, Y.; Cai, X.; Bian, Y.; Jiang, J. *Struct. Bonding (Berlin)* **2010**, *135*, 275.

(3) (a) Martinez-Diaz, M. V.; de la Torre, G.; Torres, T. *Chem. Commun.* **2010**, *46*, 7090. (b) Li, X.; Wang, H.; Wu, H. *Struct. Bonding (Berlin)* **2010**, *135*, 229. (c) Bottari, G.; de la Torre, G.; Guldi, D. M.; Torres, T. *Chem. Rev.* **2010**, *110*, 6768.

(4) Pfeiffer, M.; Leo, K.; Zhou, X.; Huang, J. S.; Hofmann, M.; Werner, A.; Blochwitz, Nimoth. *J. Org. Electron.* **2003**, *4*, 89.

(5) (a) Bench, B. A.; Beveridge, A.; Sharman, W. M.; Diebold, G. J.; van Lier, J. E.; Gorun, S. M. *Angew. Chem., Int. Ed.* **2002**, *41*, 748. (b) Bench, B. A.; Brennessel, W. W.; Lee, H. J.; Gorun, S. M. *Angew. Chem., Int. Ed.* **2002**, *41*, 750. (c) Lee, H. J.; Brennessel, W. W.; Lessing, J. A.; Brucker, W. W.; Young, V. G.; Gorun, S. M. *Chem. Commun.* **2003**, 1576. (d) Keizer, S. P.; Mack, J.; Bench, B. A.; Gorun, S. M.; Stillman, M. J. *J. Am. Chem. Soc.* **2003**, *125*, 7067. (e) Keil, C.; Tsaryova, O.; Lapok, L.; Himcinschi, C.; Wöhrle, D.; Hild, O. R.; Zahn, D. R. T.; Gorun, S. M.; Schlettwein, D. *Thin Solid Films* **2009**, *517*, 4379.

(6) (a) Liao, M.-S.; Kar, T.; Gorun, S. M.; Scheiner, S. *Inorg. Chem.* **2004**, *43*, 7151. (b) Liao, M.-S.; Watts, J. D.; Huang, M.-J.; Gorun, S. M.; Kar, T.; Scheiner., S. *J. Chem. Theory Comput.* **2005**, *1*, 1201. (c) Liao, M.-S.; Watts, J. D.; Gorun, S. M.; Scheiner, S.; Huang, M.-J. *J. Theor. Comput. Chem.* **2008**, *7*, 541.

(7) Gerdes, R.; Lapok, L.; Tsaryova, O.; Wöhrle, D.; Gorun, S. M. *Dalton Trans.* **2009**, 1098.

(8) Moons, H; Lapok, L; Loas, A; Doorslaer, Van S.; Gorun, S. M. *Inorg. Chem.* **2010**, *49*, 8779.

(9) Mattioli, G.; Filippone, F.; Amore Bonapasta, A. *J. Phys. Chem. Lett.* **2010**, 2757.

(10) (a) Sheldrick, G. M. SADABS, Multi-Scan Absorption Correction Program, Version 2; University of Göttingen: Göttingen, Germany, 2001. (b) Sheldrick, G. M. SHELXTL, Version 6.14, Bruker AXS, Inc.: Madison, WI, 2004. (c) Spek, A. L. *J. Appl. Crystallogr.* **2003**, *36*, 7–13. (d) Cambridge Structural Database, Conquest v.1.13, Cambridge Crystallographic Data Centre, Cambridge CB2 1EZ, U.K.

(11) Barrett, P. A.; Dent, C. E.; Linstead, R. P. *J. Chem. Soc.* **1936**, 1719.

(12) Griffith, C. H.; Griffiths, M.; Walker, S.; Goldstein, P. *Mol. Cryst. Liq. Cryst.* **1976**, *33*, 149.

(13) Ziolo, R. F.; Griffiths, C. H.; Troup, J. M. *J. Chem. Soc., Dalton Trans.* **1980**, 2300.

(14) Sato, T.; Tsuneda, T.; Hirao, K. *J. Chem. Phys.* **2005**, *123*, 104307.

(15) (a) Law, K.-Y. *Inorg. Chem.* **1985**, *24*, 1778. (b) Sleven, J.; Cardinaels, T.; Binnemans, K. *Liq. Cryst.* **2002**, *29*, 1425. (c) Handa, M.; Suzuki, A.; Shoji, S.; Kasuga, K.; Sogabe, K. *Inorg. Chim. Acta* **1995**, *230*, 41. (d) Kobayashi, N.; Narita, F.; Ishii, K; Muranaka, A. *Chem.—Eur. J.* **2009**, *15*, 10173.

(16) Reichenbächer, K.; Süss, H. I.; Hulliger *J. Chem. Soc. Rev.* **2005**, *34*, 22.

(17) Xu, Y.; Shi, S. *Appl. Magn. Reson.* **1996**, *11*, 1.

(18) Catalano, V. J.; Craig, T. J. *Polyhedron* **2000**, *19*, 475.

(19) Wang, Y.; Liang, D. *Adv. Mater.* **2010**, *22*, 1521.

(20) Silver, J.; Lukes, P.; Hey, P.; Ahmet, M. T. *J. Mater. Chem.* **1991**, *1*, 881.

(21) (a) Schlettwein, D.; Tada, H; Mashiko, S. *Langmuir* **2000**, *16*, 2872. (b) Basova, T.; Plyashkevich, V.; Hassan, A. *Surf. Sci.* **2008**, *602*, 2368.

(22) Nagel, S.; Lener, M.; Keil, C.; Gerdes, R.; Łapok, Ł.; Gorun, S. M.; Schlettwein, D. *J. Phys. Chem. C*, in press.

(23) Hashimoto, S.; Isoda, S.; Kurata, H.; Lieser, G.; Kobayashi, N. *J. Porphyrins Phthalocyanines* **1999**, *3*, 585.

(24) Kasha, M.; Rawls, H. R.; Ashraf El- Bayoumi, M. *Pure Appl. Chem.* **1965**, *11*, 371.